# Simultaneous Determination of the Rates of the TCA Cycle, Glucose Utilization, α-Ketoglutarate/Glutamate Exchange, and Glutamine Synthesis in Human Brain by NMR

Graeme F. Mason, Rolf Gruetter, *Douglas L. Rothman, †Kevin L. Behar, Robert G. Shulman, and †‡Edward J. Novotny

*Departments of Molecular Biophysics & Biochemistry, *Internal Medicine, †Neurology, and ‡Pediatrics, Yale University School of Medicine, New Haven, Connecticut, U.S.A.*

**Summary:** $^{13}$C isotopic tracer data previously obtained by $^{13}$C nuclear magnetic resonance in the human brain in vivo were analyzed using a mathematical model to determine metabolic rates in a region of the human neocortex. The tricarboxylic acid (TCA) cycle rate was $0.73 \pm 0.19$ $\mu$mol min$^{-1}$ g$^{-1}$ (mean $\pm$ SD; $n = 4$). The standard deviation reflects primarily intersubject variation, since individual uncertainties were low. The rate of $\alpha$-ketoglutarate/glutamate exchange was $57 \pm 26$ $\mu$mol min$^{-1}$ g$^{-1}$ ($n = 3$), which is much greater than the TCA cycle rate; the high rate indicates that $\alpha$-ketoglutarate and glutamate are in rapid exchange and can be treated as a single combined kinetic pool. The rate of synthesis of glutamine from glutamate was $0.47$ $\mu$mol min$^{-1}$ g$^{-1}$ ($n = 4$), with 95% confidence limits of 0.139 and 3.094 $\mu$mol min$^{-1}$ g$^{-1}$; individual uncertainties were biased heavily toward high synthesis rates. From the TCA cycle rate the brain oxygen consumption was estimated to be $2.14 \pm 0.48$ $\mu$mol min$^{-1}$ g$^{-1}$ ($5.07 \pm 1.14$ ml 100 g$^{-1}$ min$^{-1}$; $n = 4$), and the rate of brain glucose consumption was calculated to be $0.37 \pm 0.08$ $\mu$mol min$^{-1}$ g$^{-1}$ ($n = 4$). The sensitivity of the model to the assumptions made was evaluated, and the calculated values were found to be unchanged as long as the assumptions remained near reported physiological values. **Key Words:** Brain metabolism—CMR$_{glc}$—CMRo$_2$—Glutamine synthesis—$^{13}$C Nuclear magnetic resonance—Tricarboxylic acid cycle.

The stable isotope $^{13}$C combined with nuclear magnetic resonance (NMR) spectroscopy allows

*Abbreviations used:* Acetyl CoA, acetyl coenzyme A; Asp, aspartate concentration; Asp*, C2- or C3-labeled aspartate concentration; CMR$_{gl}$, cerebral metabolic rate for glucose; CMRo$_2$, cerebral metabolic rate for oxygen; $G_i$, brain glucose concentration; $G_i$*, brain [1-$^{13}$C]glucose concentration; $G_o$, plasma glucose concentration; $G_o$*, plasma [1-$^{13}$C]glucose concentration; Gln, brain glutamine concentration; Gln$_4$*, C4-labeled brain glutamine concentration; Glu, brain glutamate concentration; Glu$_4$*, C4-labeled brain glutamate concentration; Glu$_3$*, C3-labeled brain glutamate concentration; $\alpha$-KG, $\alpha$-ketoglutarate concentration or $\alpha$-ketoglutarate; KG$_4$*, C4-labeled $\alpha$-ketoglutarate concentration; KG$_3$*, C3-labeled $\alpha$-ketoglutarate concentration; $L$, combined concentrations of brain lactate and pyruvate; $L$*, combined concentrations of C3-labeled lactate and pyruvate; POCE, $^1$H-observed/$^{13}$C-editing; $V_{ac}$, rate of acetyl CoA entry into the TCA cycle from acetoacetate; TCA, tricarboxylic

the noninvasive, regional measurement of single and multiple metabolic rates to be made (Cohen et al., 1980; Fitzpatrick et al., 1990; Malloy et al., 1990*b*; Mason et al., 1992*a*; Rothman et al., 1992) without the use of radioactive tracers. When $^{13}$C-labeled glucose is supplied to the brain, the $^{13}$C label enters several metabolites at multiple positions, and these isotopically labeled compounds become detectable and can be distinguished in vivo by $^{13}$C NMR spectroscopy (Behar et al., 1986; Beckmann et al., 1991; Gruetter et al., 1992*a*, 1994). The high

acid; $V_\beta$, rate of acetyl CoA entry into the TCA cycle from $\beta$-hydroxybutyrate; $V_{dil}$, rate of unlabeled influx at or after lactate; $V_g$, rate of acetyl CoA entry into the TCA cycle from glycolysis; $V_{gln}$, glutamate/glutamine cycling rate; $V_{gt}$, rate of glutamate C4 labeling; $V_{ldh}$, lactate dehydrogenase rate; $V_{out}$, net rate of lactate and pyruvate efflux; $V_{pc}$, pyruvate carboxylase rate; $V_{tca}$, rate of flow through citrate synthase; $V_x$, $\alpha$-ketoglutarate/glutamate exchange rate. (All concentrations have units of $\mu$mol g$^{-1}$ wet weight. All rates have units of $\mu$mol min$^{-1}$ g$^{-1}$ wet weight.)

chemical specificity of NMR permits the identification of $^{13}C$ label in specific positions of given compounds and allows the calculation of multiple metabolic rates and substrate concentrations simultaneously when analyzed with mathematical models (Chance et al., 1983; Mason et al., 1992a). $^{13}C$ isotopomer analysis allows the evaluation of relative metabolic rates (Cohen et al., 1979; Malloy et al., 1990a). Recent improvements in resolution (Gruetter et al., 1992b; Gruetter et al., 1994) now permit $^{13}C$ isotopomer analysis in the human brain in vivo, presented here.

Radioisotope methods use the measurement of total radioactivity incorporated into a volume of tissue to determine rates of substrate consumption. The radioactivity derived from a specific substrate or its metabolites cannot be distinguished with these techniques, so these methods often require the use of metabolically inert substrate analogues, comparative studies with compounds radioisotopically labeled at different sites (Hawkins et al., 1985), and complex mathematical and statistical methods to determine specific metabolic rates (Rapoport, 1991). Despite these formidable technical difficulties, over the past two decades these techniques have become the best methods for measuring regional metabolic rates.

$^{13}C$ isotope flows in the rat brain have been measured by the $^{1}H$-observed/$^{13}C$-editing (POCE) method in which $^{13}C$ enrichments were detected from the coupled $^{1}H$ resonances (Rothman et al., 1985; Fitzpatrick et al., 1990). These observations have been analyzed by a quantitative flow model in which the assumptions of concentrations and activities were validated by comparison with literature values. In this paper a similar modeling analysis was applied to the data of Gruetter et al. (1994) obtained from the human brain in vivo to determine the rates of the tricarboxylic acid (TCA) cycle ($V_{tca}$), the synthesis of glutamine from glutamate ($V_{gln}$), and the exchange of α-ketoglutarate (α-KG) and glutamate ($V_x$). From these rates the rates of glucose utilization ($CMR_{gl}$) and oxygen utilization ($CMRo_2$) were derived. In the following sections we first present a description of the model and show how it was used for data analysis. Second, the results of the analysis are presented. Third, the effects of possible errors arising from the assumptions of the model are assessed to evaluate the sensitivity of the calculation of $V_{tca}$ to possible errors in the input assumptions.

## METABOLIC MODEL

The time courses of $^{13}C$ fractional enrichment were modeled using mass and isotope balance equations written for individual carbon positions of metabolites as described by Mason et al. (1992a). The system of equations was adjusted to fit the $^{13}C$ NMR data to determine the metabolic rates in the human brain. The model (Fig. 1) was simplified slightly from that used by Mason et al. (1992a) for the rat brain, because of the scarcity of data about some aspects of human brain metabolism (e.g., the concentrations of metabolic intermediates); the potential effects of these simplifications are evaluated under Results Section II. The differential equations that describe each of the metabolite carbon atom positions are given in Table 1.

The model assumptions were analogous to those of Mason et al. (1992a) for the rat. (1) Metabolites in
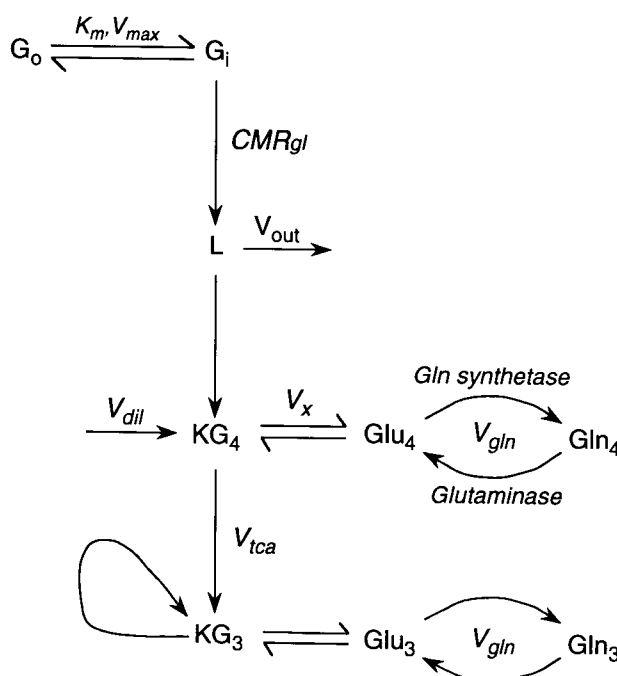


**FIG. 1.** Schematic representation of the model. Glucose in the plasma ($G_o$) and the brain ($G_i$) exchange via the Michaelis–Menten kinetic parameters $K_m$ (4.9 mM) and $V_{max}$ (3.6 × $CMR_{gl}$). Carbon flows at the rate $2CMR_{gl}$ (µmol min$^{-1}$ g$^{-1}$) through the glycolytic intermediates, assumed to have negligible concentrations, and arrives at pyruvate; pyruvate and lactate are assumed to be in isotopic equilibrium and are therefore added to form a single pool [$L$ = 0.6 µmol g$^{-1}$ (Hanstock et al., 1988)]. There is an efflux of lactate $V_{out}$ [0.12 µmol min$^{-1}$ g$^{-1}$ (calculated from Knudsen et al., 1991; Juhlin-Dannfelt, 1977)]. Unlabeled carbon enters the acetyl CoA pool to be utilized at the rate $V_{dil}$. $^{13}C$ also enters the TCA cycle at this point and labels α-KG and glutamate [9.1 µmol g$^{-1}$ (Gruetter et al., 1994)] at carbon 4, and the $^{13}C$ is exchanged between the mitochondrial and the cytosolic pools of each; these exchanges are reduced to a single exchange rate ($V_x$) between one grouped pool of glutamate (Glu$_4$) and a second grouped pool of α-ketoglutarate [α-KG$_4$ = 0.0183 × Glu$_4$ (Hawkins and Mans, 1983)]. Glutamine (4.1 µmol g$^{-1}$) is synthesized from glutamate at a rate $V_{gln}$ (µmol min$^{-1}$ g$^{-1}$). The $^{13}C$ label continues through the cycle to KG$_3$ and Glu$_3$, and on subsequent turns of the TCA cycle one-half of the label returns to KG$_3$ and Glu$_3$.

**TABLE 1.** *The differential equations that describe the model*

$dG_i/dt = V_{max}G_o/(K_m + G_o) - V_{max}G_i/(K_m + G_i) - CMR_{gl}$

$dL/dt = dKG/dt = dGlu/dt = dGln/dt = 0$

$dG_i{}^*/dt = V_{max}G_o{}^*/(K_m + G_o) - V_{max}G_i{}^*/(K_m + G_i) - CMR_{gl}(G_i{}^*/G_i)$

$dL^*/dt = CMR_{gl}(G_i{}^*/G_i) - (2CMR_{gl} + V_{out})(L^*/L)$

$dKG_4{}^*/dt = (2CMR_{gl} - V_{out})(L^*/L) + V_{dil}(0) - (V_{tca} + V_x)(KG_4{}^*/KG) + V_x(Glu_4{}^*/Glu)$

$dGlu_4{}^*/dt = V_x(KG_4{}^*/KG) - (V_x + V_{gln})(Glu_4{}^*/Glu) + V_{gln}(Gln_4{}^*/Gln)$

$dGln_4{}^*/dt = V_{gln}(Glu_4{}^*/Glu) - V_{gln}(Gln_4{}^*/Gln)$

$dKG_3{}^*/dt = \tfrac{1}{2}V_{tca}(KG_4{}^*/KG) - \tfrac{1}{2}V_{tca}(KG_3{}^*/KG) - V_x(KG_3{}^*/KG) + V_x(Glu_3{}^*/Glu)$

$dGlu_3{}^*/dt = V_x(KG_3{}^*/KG) - (V_x + V_{gln})(Glu_3{}^*/Glu) + V_{gln}(Gln_3{}^*/Gln)$

$dGln_3{}^*/dt = V_{gln}(Glu_3{}^*/Glu) - V_{gln}(Gln_3{}^*/Gln)$

A superscript asterisk denotes molecules labeled with $^{13}C$ at the carbon position denoted by the subscripted number.

rapid chemical and isotopic exchange were represented by a single kinetic pool whose concentration equals the sum of its constituents. (2) Glucose provided the only $^{13}C$-labeled carbon substrate for the TCA cycle. (3) Gluconeogenesis was negligible in the human brain, as shown in the rat brain (Hawkins and Mans, 1983). (4) The subjects were sensory-deprived to minimize chance stimulation and hence the system was in a metabolic steady state throughout the experiment. Previous $^1H$ NMR measurements during glucose infusions in rats (Fitzpatrick et al., 1990) and humans (Rothman et al., 1992) have shown that the total concentrations of all detectable metabolites except glucose were constant. (5) Glutamate was the precursor for glutamine synthesis. (6) Glutamate was assumed to behave as a single kinetic pool, indistinguishable from a small pool and a large pool. (7) Isotopic exchange among the mitochondrial and cytosolic pools of $\alpha$-KG and glutamate were represented as a single exchange reaction described by the rate $V_x$ (Mason et al., 1992a). This was one of the three rates determined by fitting the data with the model. The other two were the TCA cycle rate and $V_{gln}$.

Two of the assumptions differed from those made previously for the rat brain: (a) Glucose transport was limited by the blood–brain barrier and transport kinetics were described by the symmetric Michaelis–Menten model using kinetic constants determined in human brain by Gruetter et al. (1992a) using $^{13}C$ NMR, whereas glucose transport was assumed to be infinitely fast in the rat brain. (b) Small pools of glycolytic and TCA cycle intermediates were neglected.

The values of $V_{tca}$, $V_x$, and $V_{gln}$ were adjusted iteratively by computer to obtain the best fits to the data. Inputs for the modeling analysis are categorized either as data measured in the NMR experiment or as previously published data. Data from the

NMR experiments (Gruetter et al., 1993) consisted of (a) the measured time courses of the plasma glucose concentration and its 1-$^{13}C$ fractional enrichment, (b) the time courses of the C4 and C3 enrichments of glutamate and the C4 label concentrations of glutamate and glutamine, (c) the total ($^{12}C + ^{13}C$) concentrations of glutamate and glutamine, (d) the steady-state fractional enrichment of glutamate C4, and (e) an upper limit of 0.1 $\mu mol\ g^{-1}$ for the concentration of $\alpha$-KG because its NMR signal was too low to detect; Howse and Duffy (1975) reported a concentration of 0.1 $\mu mol\ g^{-1}$ for the rat brain and showed that aspartate aminotransferase was in thermodynamic equilibrium. Data from previously published measurements consisted of (a) blood–brain glucose transport kinetics (Gruetter et al., 1992a), (b) the concentration of brain lactate measured by $^1H$ NMR (Hanstock et al., 1988), and (c) the rate of lactate efflux from the brain (Juhlin-Dannfelt, 1977; Knudsen et al., 1991).

## METHODS

This section describes the stepwise procedure for fitting the model to the data to derive each parameter.

The present work is a detailed analysis of data obtained by Gruetter et al. (1994), who infused [1-$^{13}C$]glucose into healthy adult volunteers over periods of 2–3 h. During the infusions, carbons 3 and 4 of glutamate and glutamine were labeled with $^{13}C$, and direct $^{13}C$ detection with $^1H$ decoupling was used to detect the glutamate and glutamine labeling time courses. At isotopic steady state, fractional $^{13}C$ enrichments and concentrations were determined for glutamate and glutamine. The time courses of $^{13}C$ glucose fractional enrichments were measured by gas chromotography–mass spectrometry and $^1H$ NMR spectroscopy at 360 MHz (Behar et al., 1986; Mason et al., 1992b). More technical details of the data acquisition and analysis are described by Gruetter et al. (1994). The time courses of the glutamate C4, glutamate C3, and glutamine C4 concentrations and the C4 and C3 enrichments of glutamate were analyzed in the present work. The assumed metabolite concentrations and rates are given in the legend to Fig. 1. The modeling analysis was implemented on a 33-MHz 486 personal computer (Dell 433E, Austin, TX, U.S.A.) with Turbo Pascal 3.0 (Borland International, Inc., Scotts Valley, CA, U.S.A.), using a Runge–Kutta method to solve the differential equations and a modified simplex algorithm to iterate the parameters to find best fits as reported previously (Mason et al., 1992a). The 200 min of experimental data were divided into 1,000–32,000 intervals for the numerical integration of the differential equations.

A three-step procedure was used to determine the values of $V_{gln}$, $V_{tca}$, and $V_x$. (1) The NMR-measured time courses of glutamine C4 and glutamate C4 were compared to determine the value of $V_{gln}$. (2) The time course of glutamate C4 was analyzed with respect to the plasma glucose concentration and 1-$^{13}C$ enrichment time courses to determine the rate of glutamate C4 turnover ($V_{gt}$). (3) The time courses of glutamate C4 and glutamate C3 en-

richment were compared to determine $V_x$ and $V_{tca}$. These three steps are described in detail in the following.

The numerical method used to determine uncertainties in iterated parameters was described by Mason et al. (1992a). The method translated the signal-to-noise ratios of the data into standard deviations about the expected value for the parameters iterated. The same method is also applied here to determine 95% confidence intervals for the nonnormally distributed parameter $V_{gln}$.

## Determination of the rate $V_{gln}$

In a single-compartment model, glutamine is formed from glutamate and is consistent with Fig. 1. On this basis the glutamate C4 time course was used as the input function for the analysis of the glutamine C4 time course. The expression for $dGln_4*/dt$ in line 7 in Table 1 was fitted to the glutamine C4 time courses from Gruetter et al. (1994) to determine the value of $V_{gln}$.

Based on enzymatic and isotopic data, glutamine is believed to be synthesized from a small pool of glutamate exclusively in a second compartment (for review see Cooper and Plum, 1987). Since in vivo glutamine C4 was observed to be labeled almost as rapidly as glutamate C4 (Gruetter et al., 1994), a two-compartment analysis must permit either (1) rapid transport and uptake of labeled glutamate and conversion to glutamine, which is mathematically identical to the one-compartment model, or (2) rapid labeling of glutamine from a small pool of glutamate labeled by [1-$^{13}$C]glucose, which yields the same TCA cycle rate as the model in Fig. 1 (this is demonstrated under Discussion).

## Determination of $V_{gt}$

Gruetter et al. (1994) observed a small decrease in the steady-state fractional enrichments of glutamate C4 compared to the theoretical value (one-half of the plasma glucose 1-$^{13}$C enrichment). This dilution was explained by the pentose phosphate shunt flux and the influx of unlabeled substrates from the blood, as discussed later. The dilution is described in the model by a rate of isotopic dilution $V_{dil}$. The reported dilution cannot be caused by metabolically inactive pools, since the isotopomer analysis used by Gruetter et al. (1994) measures the enrichments of pools of metabolites that are labeled by glucose. However, the agreement of the concentrations of glutamate and glutamine with previously reported values indicates that essentially all of these two pools turn over rapidly and are metabolically active. To determine $V_{dil}$ relative to $V_{gt}$, the steady-state fractional enrichments of glutamate C4 and [1-$^{13}$C]glucose were compared. For a given plasma [1-$^{13}$C]glucose enrichment $G_o*/G_o$, the steady state glutamate C4 enrichment expected would be $\frac{1}{2}G_o*/G_o$ if $V_{dil}$ were zero, so

$$V_{dil}/V_{gt} = 1 - (Glu_4*/Glu)/(\frac{1}{2}G_o*/G_o) \qquad (1)$$

Equation 1 was used to calculate the value of $V_{dil}/V_{gt}$, and the simplified model in Fig. 2 was fitted to the glutamate C4 time course for each subject by iteration of the value of $V_{gt}$.

## Determination of $V_{tca}$ and $V_x$ from glutamate C4 and glutamate C3 data

As described by Mason et al. (1992a), the ratio $V_x/V_{tca}$ can be evaluated by comparison of the glutamate C4 and

glutamate C3 labeling time courses. The relationship between $V_{gt}$ and the metabolic rates $V_x$ and $V_{tca}$ is

$$V_{tca} = V_{gt}\left(\frac{1 + (V_x/V_{tca})}{V_x/V_{tca}}\right) \qquad (2)$$

To determine the values of $V_{tca}$ and $V_x/V_{tca}$ from $V_{gt}$, the ratio $V_x/V_{tca}$ was iterated to fit the model to the glutamate C3 enrichment data. The value of $V_{tca}$ was calculated for each subject with Eq. 2, using the individual's values of $V_{gt}$ and $V_x/V_{tca}$. The value of $V_x$ was then calculated from $V_{tca}$ and $V_x/V_{tca}$.

## RESULTS, SECTION I

### Glutamine synthesis

Given a concentration of glutamine of 4.1 ± 0.3 μmol g$^{-1}$ [mean ± SD, $n = 4$ (Gruetter et al., 1994)], the average value of $V_{gln}$ for the four subjects was 0.47 μmol min$^{-1}$ g$^{-1}$ (95% confidence interval = 0.139–3.094 μmol min$^{-1}$ g$^{-1}$; Table 2 and Fig. 3). The individual distributions of $V_{gln}$ determined from the scatter analysis were not normal and spread toward high numbers, because high values of $V_{gln}$ yielded fits that were similar in quality. For example, the goodness of fit using a value of $V_{gln} = 0.1$ μmol min$^{-1}$ g$^{-1}$ was similar to the good-
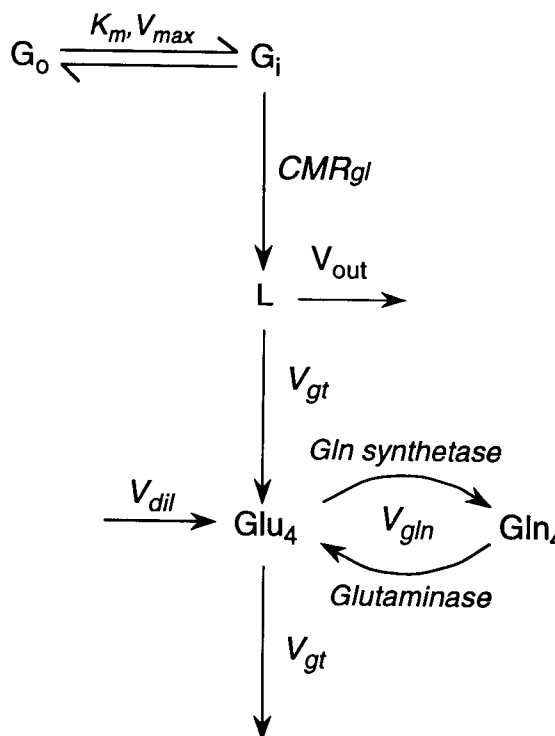


FIG. 2. Schematic representation of the model used to calculate the rate of glutamate turnover ($V_{gt}$). The TCA cycle rate and the α-KG/glutamate exchange rate were combined and replaced with $V_{gt}$. C3-labeled products were irrelevant for the calculation of $V_{gt}$ and are not shown in this schematic.

**TABLE 2.** *The $V_{gln}$ and $V_{gt}$ for each of the four volunteers*

| $i$ | $V_{gln}$ ($\mu$mol min$^{-1}$ g$^{-1}$) | $V_{gt}$ ($\mu$mol min$^{-1}$ g$^{-1}$) |
|---|---|---|
| 1 | 0.582 (0.172–3.272) | 0.906 ± 0.226 |
| 2 | 0.742 (0.185–6.581) | 0.515 ± 0.029 |
| 3 | 0.402 (0.144–2.173) | 0.819 ± 0.056 |
| 4 | 0.139 (0.053–0.349) | 0.628 ± 0.055 |
| Mean | 0.466 (0.139–3.094) | 0.718 ± 0.178 |

To determine $V_{gln}$, the model was fit to the glutamine C4 time courses using the glutamate C4 time course as input functions. The 95% confidence limits for $V_{gln}$, given in parentheses, were calculated from the signal-to-noise ratios of the glutamine C4 NMR time courses. The model was then fitted to the glutamate C4 time courses (Gruetter et al., 1994) to obtain $V_{gt}$. The uncertainties in $V_{gt}$ for each volunteer are standard deviations calculated from the scatter of the data about the calculated best fit of the model to the glutamate C4 data. The bottom of column 2 shows the mean value of $V_{gln}$ with average 95% confidence limits, and the bottom of column 3 shows the mean value of $V_{gt}$ ± SD for the four volunteers.

ness of fit using a value of $V_{gln}$ = 4.0 $\mu$mol min$^{-1}$ g$^{-1}$. This behavior occurred because the glutamine C4 time course followed the glutamate C4 time course closely, and once the calculated exchange was fast enough to cause the predicted glutamine C4 labeling to follow the fractional glutamate C4 labeling closely, faster exchange rates did not alter the glutamate/glutamine labeling relationship significantly.

### Glutamate C4 turnover rate

Using the measured values of glutamate C4 and [1-$^{13}$C]glucose fractional enrichments of 27 ± 2 and 63 ± 1%, respectively (mean ± SD; $n$ = 4) (Gruetter et al., 1994), the calculated value of $V_{dil}$ was 14.3 ± 3.3% of $V_{gt}$ ($n$ = 4). Given a concentration of 9.1 ± 0.7 $\mu$mol g$^{-1}$ ($n$ = 4) for glutamate (Gruetter et al., 1994), the value of $V_{gt}$ was calculated to be 0.718 ± 0.178 $\mu$mol min$^{-1}$g$^{-1}$ ($n$ = 4; Table 2).
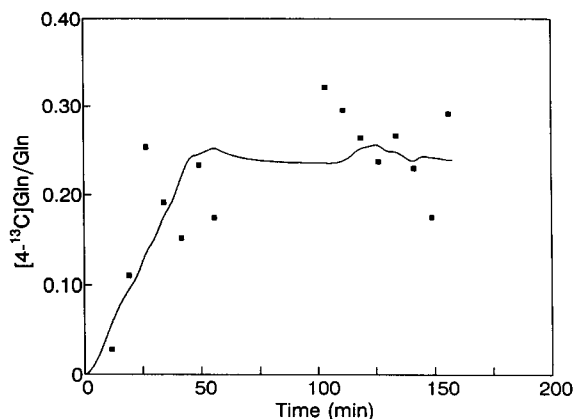


**FIG. 3.** Fit of the model to the time course of glutamine C4. The fit shows bumps and waves that reflect the behavior of the glutamate C4 time course that was used as input.

### Glutamate C4 and glutamate C3 time course comparison

Fits to data from the same experiment as the data in Fig. 3 are shown in Fig. 4A and B, and the results for all four subjects are given in Table 3. The calculation yielded values of $V_{tca}$ = 0.729 ± 0.185 $\mu$mol min$^{-1}$ g$^{-1}$ (mean ± SD; $n$ = 4) and $V_x$ = 57 ± 26 $\mu$mol min$^{-1}$ g$^{-1}$ ($n$ = 3). Since $V_x/V_{tca} \gg 1$, the glutamate effectively acts as a label trap and the rate of glutamate C4 label formation is equivalent to the value of $V_{tca}$. This validation was previously obtained for N$_2$O-anesthetized rats (Mason et al., 1992a). The individual experimental uncertainty in $V_{tca}$ due to noise in the NMR data was only 6–9% for subjects 2–4. The uncertainty for subject 1 was higher (24%) because fewer glutamate C4 data were acquired near steady state.

The value of $V_{tca}$ is influenced by the rate of interconversion of glutamate and glutamine through
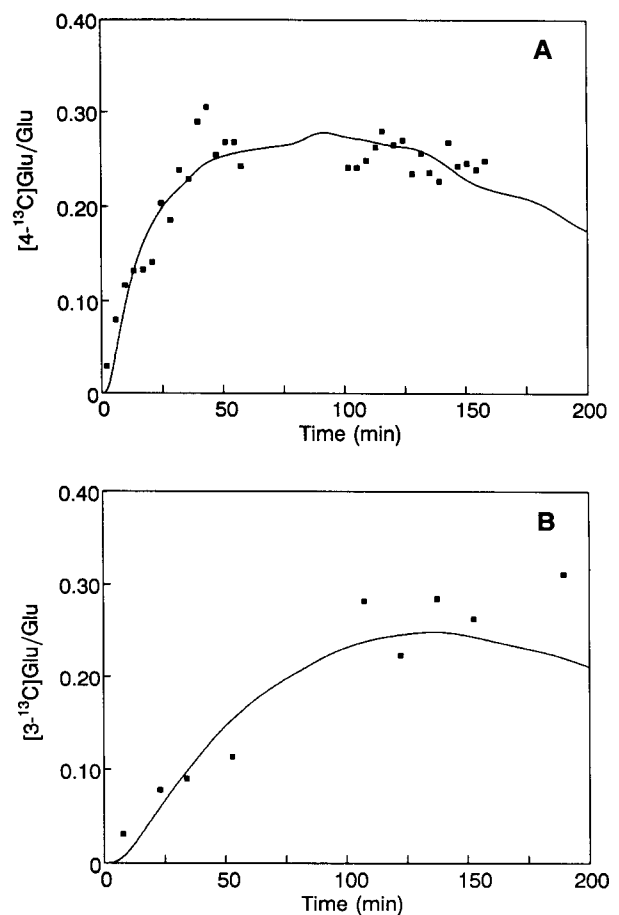


**FIG. 4.** Fits of the model to the time courses of **(A)** glutamate C4 and **(B)** glutamate C3 in the same subject as in Fig. 3. The fits to glutamate C4 and glutamate C3 are smoother than the fit to glutamine C4 (Fig. 3). Bumps and waves in the input function (plasma glucose) were smoothed by intervening metabolite pools; the smoothing was a consequence of the damping nature of the first-order kinetic equations in Table 1.

**TABLE 3.** *Determination of* $V_x/V_{tca}$ *and* $V_{tca}$

| $i$ | $V_x/V_{tca}$ | $V_{tca}$ ($\mu$mol min$^{-1}$ g$^{-1}$) | $V_x$ ($\mu$mol min$^{-1}$ g$^{-1}$) | CMR$_{gl}$ ($\mu$mol min$^{-1}$ g$^{-1}$) |
|---|---|---|---|---|
| 1 | 45 | 0.926 ± 0.231 | 42 | 0.458 ± 0.116 |
| 2 | — | 0.522 ± 0.029 | — | 0.284 ± 0.015 |
| 3 | 49 | 0.836 ± 0.057 | 41 | 0.419 ± 0.029 |
| 4 | 136 | 0.633 ± 0.056 | 87 | 0.332 ± 0.028 |
| Mean ± SD | 77 ± 51 | 0.729 ± 0.185 | 57 ± 26 | 0.373 ± 0.079 |

The model in Fig. 1 was fitted to the glutamate C3 time courses to obtain the values for $V_x/V_{tca}$, using the values of $V_{gln}$, glutamate, $V_{gt}$, and glutamine determined for each subject. The individual uncertainties are standard deviations calculated from the scatter of the data about the calculated best fit of the model in Fig. 1 to the glutamate C3 time course. The value of $V_{tca}$ for subject 2 was calculated using the average $V_x/V_{tca}$ value from subjects 1, 3, and 4. CMR$_{gl}$ was calculated from the relationship between glycolysis and the TCA cycle rate, shown in Fig. 1 and described under Discussion.

the combined actions of glutamine synthetase and glutaminase ($V_{gln}$), because this interconversion forces some of the label that passes through glutamate to spend time in the glutamine pool. If $V_{gln}$ were very fast, then the $^{13}$C would label both glutamate and glutamine as if they were a single metabolic pool. If $V_{gln}$ were very slow, then glutamine would have a negligible influence on the glutamate C4 time course. Since the glutamine C4 time course lags the glutamate C4 time course slightly but significantly, we know that neither extreme is the case. Because the value of $V_{gln}$ (0.47 $\mu$mol min$^{-1}$ g$^{-1}$) had a broad distribution biased toward high values (95% confidence interval = 0.139–3.094 $\mu$mol min$^{-1}$ g$^{-1}$; Table 2), the effects of a range of values of $V_{gln}$ upon the determination of $V_{tca}$ and the concentration of glutamate were evaluated (Table 4). It was found that once the value of $V_{gln}$ was 0.20 $\mu$mol min$^{-1}$ g$^{-1}$ or higher, the deviation of $V_{tca}$ from 0.718 $\mu$mol min$^{-1}$ g$^{-1}$ was ~8% or less (an amount equal to or less than the experimental uncertainty).

## RESULTS, SECTION II

The model included a number of parameters whose values were assumed. In this section, the

**TABLE 4.** *The effect of glutamate/glutamine exchange on the determination of* $V_{tca}$

| $V_{gln}$ ($\mu$mol min$^{-1}$ g$^{-1}$) | $V_{tca}$ ($\mu$mol min$^{-1}$ g$^{-1}$) | $V_{tca}$ error (%) |
|---|---|---|
| 0.053 | 0.888 | 21.6 |
| 0.125 | 0.833 | 14.0 |
| 0.205 | 0.791 | 8.3 |
| 0.410 | 0.739 | 1.2 |
| 0.466 | 0.729 | 0.0 |
| 2.050 | 0.683 | −6.4 |
| 4.100 | 0.790 | −7.3 |
| 6.581 | 0.674 | −7.6 |

Glutamate C4 time courses were simulated using $V_{tca}$ = 0.729 $\mu$mol min$^{-1}$ g$^{-1}$ with a range of values for $V_{gln}$ (column 1). The simulated time courses were used as input for the model's fitting procedure to determine $V_{tca}$ (column 2) and the percentage differences were calculated (column 3).

sensitivity of the calculated values of $V_{tca}$ to these parameters is investigated. The parameters are quantities whose values have been assumed based on previously published studies. The conclusion of the testing was that the effects of all of these assumptions on the determination of $V_{tca}$ are small and do not significantly affect the rates derived using the model within and, in some cases, beyond the extremes of previously reported values. The following assumptions were evaluated: (a) brain glucose transport, (b) neglect of glycolytic and TCA cycle intermediates, (c) assumption of a very fast lactate/pyruvate exchange, (d) net flux of lactate, pyruvate, and ketone bodies, (e) pyruvate carboxylase rate, and (f) recycling of $^{13}$C label to glucose positions other than C1. In addition, the range of TCA cycle rates that could be measured precisely was determined from simulations, and the method was found to retain its precision over a broader range than is expected to occur in vivo.

A numerical approach was unnecessary for some assumptions, but for most the numerical evaluations were performed. The numerical evaluation was designed to answer the question, "What value of $V_{tca}$ would be derived using the model with all its assumptions if a given test parameter were varied within or in some cases beyond the extremes of previously reported values?" The algorithm of the test had two steps. (1) The value of $V_{tca}$ equal to the average from the four subjects (0.729 $\mu$mol min$^{-1}$ g$^{-1}$) was used to simulate a noiseless glutamate C4 labeling time course for each value of the assumed parameter over the test range. Simulated time courses were used instead of actual data because small sensitivities would be hidden by the effects of noise in the data. (2) The original assumptions were used to calculate best fit values of $V_{tca}$ from the simulated time courses.

**Brain glucose transport**

The time required for brain glucose to reach isotopic equilibrium with plasma glucose can be de-

scribed by the term $\Delta t_{1/2}$, which is the difference between the times required for the [1-$^{13}$C]glucose infusion to raise the plasma and brain glucose fractional 1-$^{13}$C enrichments to one-half of their steady-state levels. The primary effects of glucose transport on the calculation of $V_{tca}$ are described by the parameter $\Delta t_{1/2}$. Glucose transport kinetic constants of 4.9 m$M$ for $K_m$ and 3.6 for $V_{max}$/CMR$_{gl}$ determined by $^{13}$C NMR (Gruetter et al., 1992$a$) with a TCA cycle rate $V_{tca} = 0.729$ $\mu$mol min$^{-1}$ g$^{-1}$ led to a value of 1.50 min for $\Delta t_{1/2}$ during a typical [1-$^{13}$C]glucose infusion protocol. The glucose transport kinetics of Vyska et al. (1985) and Feinendegen et al. (1986) measured using positron emission tomography (PET) in humans yielded similar $\Delta t_{1/2}$ values (1.55 and 1.45 min, respectively). The smallest value of $\Delta t_{1/2}$ assumed in the test was 0, which corresponded to infinitely fast blood–brain glucose transport. The largest value of $\Delta t_{1/2}$ assumed in the test was 2.6 min, which corresponded to unidirectional flow at the rate CMR$_{gl}$ (0.37 $\mu$mol min$^{-1}$ g$^{-1}$; see Discussion) through a brain glucose pool of 1.0 $\mu$mol g$^{-1}$ (Gruetter et al., 1992$a$); since at the beginning of the [1-$^{13}$C]glucose infusion the brain glucose pool increases in concentration as well as in isotopic enrichment, the true value of $\Delta t_{1/2}$ must be lower than 2.6 min.

Time courses of glutamate C4 labeling were simulated using a range of $\Delta t_{1/2}$ values between the two extremes. The simulated time courses were then used as input for the model's fitting procedure, and values of $V_{tca}$ were calculated. For $\Delta t_{1/2}$ of 0.5 min, the value of $V_{tca}$ would be overestimated by 8.8%. If $\Delta t_{1/2}$ were 1.0 or 2.0 min, the error in $V_{tca}$ would lie between $-4.5$ and $-5\%$. Since most data indicate that $\Delta t_{1/2}$ lies within 30 s of the present model's value of 1.5 min (calculated from Vyska et al., 1985; Feinendegen et al., 1986; Gruetter et al., 1992$a$), very little error in $V_{tca}$ is introduced by deviations from the values of the glucose transport kinetic constants.

### Neglect of glycolytic and TCA cycle intermediates

The glycolytic intermediates were assumed to be low in concentration relative to the carbon flux and therefore to have such short isotopic equilibration times that they could be neglected. To evaluate the effect of this assumption on the calculation of $V_{tca}$, glutamate C4 labeling time courses were simulated for a range of concentrations. The simulated labeling time courses were then used as input for the model's fitting procedure. Since little information on glycolytic intermediates in the human brain is available, the upper extreme for testing was 0.28 $\mu$mol g$^{-1}$, which is the sum of the concentrations in

the rat brain (Hawkins and Mans, 1983). The concentrations of brain metabolites are usually higher in the rat (Hawkins and Mans, 1983; Petroff et al., 1989), so the values from the rat probably represent an extreme case for this test. The value of $V_{tca}$ derived from the simulated time courses neglecting intermediates was within 2.5% of the value of $V_{tca}$ calculated at the upper test extreme.

Variations in the concentrations of TCA cycle intermediates that follow $\alpha$-KG have only a slight impact on the value of $V_x$ (Mason et al., 1992$a$), which yields a negligible effect on the value of $V_{tca}$.

### Exchange between lactate and pyruvate

The concentration of lactate is much higher than the concentrations of the glycolytic intermediates. If lactate and pyruvate are in fast exchange, as assumed in the model, the $^{13}$C labels the lactate pool before the TCA cycle intermediates and glutamate; since the concentration of lactate is appreciable [0.6 $\mu$mol g$^{-1}$ (Hanstock et al., 1988)], fast exchange will delay the arrival of the label in glutamate, forcing the model calculation to compensate with a higher value of $V_{tca}$ than would be the case for slow lactate/pyruvate exchange. The delay is analogous to the lag between glutamate C4 and glutamate C3 labeling, which was caused by rapid exchange of $\alpha$-KG and glutamate.

To test the sensitivity of the calculation of $V_{tca}$ to the value of $V_{ldh}$, glutamate C4 time courses were simulated using a range of values of the ratio $V_{ldh}$/$V_{tca}$ from a minimum of 0.0 to a maximum of infinity, which was the value used for the data analysis. For testing it was assumed that the lactate:pyruvate ratio in the human brain is the same as in the rat brain [15:1 (Hawkins and Mans, 1983)]. When $V_{ldh}$/$V_{tca} = 0$, $V_{tca}$ was 4.7% higher than for a ratio of infinity; when $V_{ldh}$/$V_{tca} > 2$, the error in the derived value of $V_{tca}$ was less than 0.01%. Since $V_{ldh}$/$V_{tca}$ has been reported to be $\sim$100 in the rat brain (Lowry and Passonneau, 1964; Balázs, 1970), the assumption of fast exchange between pyruvate and lactate is expected to have no significant effect on the calculation of $V_{tca}$ determined from the data.

### Net blood–brain exchange of lactate, pyruvate, and ketone bodies

Deviations of the net flux of these metabolites can change the relationship of CMR$_{gl}$ and $V_{tca}$ that was assumed in the model. Arterial-difference measurements in humans have yielded net lactate and pyruvate efflux values totaling 9–10% of CMR$_{gl}$ (Gottstein et al., 1963; Juhlin-Dannfelt, 1977) and net ketone body influx values of 9.8% of CMR$_{gl}$ (Juhlin-Dannfelt, 1977). The net carbon flux expected from these values of lactate efflux and ke-

tone body influx would therefore compensate each other closely, with a net influx of 0.8% of $CMR_{gl}$.

The model was tested for net carbon transfer rates ranging from influx of 10% of $V_{tca}$ to efflux of 20% of $V_{tca}$, with errors in $V_{tca}$ ranging from over-estimation of 0.1% to underestimation of 6.0%. The test showed that the value of $V_{tca}$ has negligible sensitivities to changes in the net fluxes of lactate, pyruvate, and ketone bodies.

**Pyruvate carboxylase rate**

Pyruvate carboxylase exerts its effect on the calculation of $V_{tca}$ in two ways. One affects the values of $V_{tca}$ and glutamate by altering the relationship between $V_{tca}$ and $CMR_{gl}$, and the other affects the $V_x/V_{tca}$ determination.

The alteration of the $V_{tca}:CMR_{gl}$ relationship is mathematically the same as discussed for net carbon fluxes into and out of the TCA cycle. In the rat brain the pyruvate carboxylase rate ($V_{pc}$) has been reported to be 10% of $V_{tca}$ (Berl et al., 1962), and the testing of net carbon transfer showed that fluxes of 20% of $CMR_{gl}$ (~10% of $V_{tca}$) have a negligible impact on the determination of $V_{tca}$ and glutamate.

The second effect of pyruvate carboxylase occurs because the path leads to the formation of glutamate C3 instead of glutamate C4. This causes the gluta-mate C3 time course to rise more rapidly than would be expected if $V_{pc}$ were zero. The calculation of $V_x/V_{tca}$ depends on the lag of glutamate C3 be-hind glutamate C4, and a smaller lag leads to the calculation of a lower value of $V_x$. Therefore, if pyruvate carboxylase activity is appreciable, the model actually underestimates the α-KG/glutamate exchange rate. Since the value of $V_x$ is already very large, the C3 labeling aspect of the assumption of a higher value for $V_{pc}$ would have a negligible effect on the calculation of $V_{tca}$.

**¹³C recycling**

The recycling of isotopically labeled carbon at-oms in glucose due to systemic metabolism and re-synthesis by the liver can result in a redistribution of the isotope in the glucose molecule (Katz and Rognstad, 1976). Recycling of ¹³C from C1 to C6 of glucose would contribute to the labeling of gluta-mate C4, so C1–C6 recycling has the same effects as increasing the glucose 1-¹³C fractional enrichment. If significant glucose C6 labeling were neglected, the value of glutamate determined by Gruetter et al. (1994) would be an overestimate and would cause $V_{tca}$ to be overestimated as well, since the determi-nation of $V_{tca}$ depends on the quantification of glu-tamate.

The fractional ¹³C labeling of C2–C6 of plasma glucose as measured in pentacetate derivatives by gas chromatographic mass spectrometry (Shulman et al., 1990) was less than 0.5% in all subjects, in-cluding subject 4, whose [1-¹³C]glucose infusion was of the longest duration (3.5 h). Even if all of the recycled ¹³C went to C6, there would be no detect-able effect on the calculation of glutamate or $V_{tca}$.

**Precision as a function of the value of $V_{tca}$**

Fast and slow extremes of $V_{tca}$ change the amount of data that can be acquired before the glu-tamate C4 reaches an isotopic steady state and can therefore affect the precision of the determination of $V_{tca}$. We tested the model to determine where the limits of precision are for slow and fast extremes of $V_{tca}$. For low values of $V_{tca}$, the ¹³C labeling time courses take longer to reach a steady state, which allows more time to acquire NMR data and thereby improves precision. However, if the value of $V_{tca}$ falls enough that the Glu C4 and C3 do not reach isotopic steady state for accurate measurement of the glutamate C4 steady-state labeling, fractional enrichment, and pool size, the measurement of the glutamate pool size will be more uncertain and the accuracy of the calculation of $V_{tca}$ will decrease. Simulations show that for a glutamate concentra-tion of 9.1 μmol $g^{-1}$ and an experimental duration of 180 min, the TCA cycle must operate at least as fast as 0.05 μmol $min^{-1}$ $g^{-1}$, or 7% of its normal value, for the glutamate C4 and C3 labeling to reach 95% of an isotopic steady state. As an approxima-tion, the minimum measurable value of $V_{tca}$ is di-rectly proportional to the concentration of gluta-mate.

For high values of $V_{tca}$, the glutamate C4 reaches an isotopic steady state quickly, which leaves less time to acquire NMR data during non-steady-state conditions and decreases the accuracy of the deter-mination of $V_{tca}$. To determine the range of precise determination of $V_{tca}$, simulated data were gener-ated with various rates of $V_{tca}$, using the same noise levels that were achieved in the actual studies. The precision of the calculated value of $V_{tca}$ was better than 9% for values of $V_{tca}$ of up to three times the average value of $V_{tca}$ determined in this study, or 2.25 μmol $min^{-1}$ $g^{-1}$. These calculations demon-strate that $V_{tca}$ can be precisely determined for rates well beyond those expected in the human brain in vivo.

**DISCUSSION**

We have analyzed the data of Gruetter et al. (1993) with a metabolic model and have determined the $V_{tca}$, $CMR_{gl}$, $V_{gln}$, and $V_x/V_{tca}$. Individual uncertain-

ties were calculated from the signal-to-noise ratios and, for $V_{tca}$, were much smaller than the uncertainties for the group, so the NMR measurements were sensitive enough to detect intersubject variations in the value of $V_{tca}$.

The sensitivities of the model to the assumptions used in its formation were evaluated within limits provided in the literature. Errors that would be introduced by changes in the values of parameters in the model (e.g., slower exchange between pyruvate and lactate) were evaluated and found to have negligible effects on the calculation of the TCA cycle rate. In other words, errors caused by deviations from the assumptions in the model were smaller than the individual uncertainties caused by noise in the data. By this method the model was found to be very robust.

### $CMR_{gl}$

The $CMR_{gl}$ was calculated from the $V_{tca}$ for each subject using mass balance at the α-KG pool in Fig. 1, so that $CMR_{gl} = \frac{1}{2}(V_{tca} + V_{dil} - V_{out})$. The results yielded a mean value of $CMR_{gl} = 0.37 \pm 0.08$ μmol min$^{-1}$ g$^{-1}$ (mean ± SD, $n = 4$; Table 3). This rate lies in the ranges of previously reported values of 0.40 determined by PET for the occipital cortex (Heiss et al., 1984; Tyler et al., 1988) and 0.33 μmol min$^{-1}$ g$^{-1}$ globally in the gray matter (Phelps et al., 1979) using fluorodeoxyglucose and 0.23 to 0.39 μmol min$^{-1}$ g$^{-1}$ determined with arterial–venous difference and blood flow measurements (Gottstein et al., 1963).

Our value of $CMR_{gl}$ was determined from a 144-cm$^3$ volume of predominantly gray matter in the occipital region of the brain. Heiss et al. (1984) reported values of $CMR_{gl}$ in occipital gray and white matter of 0.401 and 0.17 μmol min$^{-1}$ g$^{-1}$, respectively, which lead to an estimate that the present data arise from ~90% gray matter.

### Sources of isotopic dilution

While glucose is the primary source of carbon for the TCA cycle, and the majority of that carbon arrives via glycolysis, other substrates and pathways contribute predominantly unlabeled carbon to the TCA cycle. These alternate pathways are important both because of the dilution effects they introduce at glutamate C4 and because of potential effects on the proportionality between $V_{tca}$ and $CMR_{O_2}$. First we address the issue of label dilution.

As stated earlier, the measured fractional enrichment of glutamate C4 was less than would be the case if glucose were the only substrate for the synthesis of glutamate. There was a 14.3 ± 3.3% dilution of glutamate C4 (mean ± SD), and this dilution presumably included contributions from the pen-

tose phosphate shunt, degradation of proteins, and influx of unlabeled lactate, pyruvate, and ketone bodies from the blood. The rate of protein degradation is negligible in rats [0.3% of $V_{tca}$ (calculated from Berl et al., 1961)] and is probably slower in humans. Knudsen et al. (1991) reported a value of 0.08 ± 0.03 μmol min$^{-1}$ g$^{-1}$ ($n = 18$) for the unidirectional influx of lactate in humans, which corresponds to a contribution of 10 ± 3% to the carbon flux into the TCA cycle. The pentose phosphate shunt causes label dilution by cleavage of the $^{13}C$ isotope from [1-$^{13}$C]glucose and is reported to operate at 1–3% of $CMR_{gl}$ in the rat brain (Gaitonde et al., 1983; Hawkins et al., 1985), which, for our results, means a dilution rate of 0.0037–0.0111 μmol min$^{-1}$ g$^{-1}$.

No information about the unidirectional uptake of pyruvate in the human brain was available, but in the rat brain pyruvate transport is much slower than lactate transport (Pardridge and Oldendorf, 1977) and is expected to have a negligible contribution to unidirectional uptake in the human brain.

No information about the unidirectional uptake of ketone bodies in the human brain was available, but if one assumes that brain ketone body production is negligible, then the rate of ketone body consumption is equal to the rate of net influx. The net rates of acetoacetate and β-hydroxybutyrate influx, calculated from the arterial-difference measurements of Juhlin-Dannfelt (1977), are 0.86 ± 0.29 and 4.00 ± 1.57% of $CMR_{gl}$, respectively ($n = 7$), which correspond to influx rates of 0.0032 ± 0.0013 and 0.0148 ± 0.0066 μmol min$^{-1}$ g$^{-1}$. Since each unit of ketone body produces 2 units of acetyl CoA, the total rate of isotopic dilution due to ketone bodies is 0.036 ± 0.013 μmol min$^{-1}$ g$^{-1}$.

The total dilution expected from all sources is then 0.13 ± 0.033 μmol min$^{-1}$ g$^{-1}$, which is 17.8 ± 4.5% of $V_{tca}$. This predicted percentage of dilution is close to the measured value of 14.3 ± 3.3% ($n = 4$) determined from the measurements (Gruetter et al., 1994). It therefore seems likely that the pentose phosphate shunt and lactate and ketone body influx are responsible for the dilution of glutamate C4 fractional enrichment, with the lactate influx as the dominant factor.

### $CMR_{O_2}$

If glucose were the only substrate for oxidative metabolism, the values of $V_{tca}$ and $CMR_{O_2}$ would be directly proportional. However, ketone bodies yield different amounts of reducing power and thereby alter the proportionality. The value of the TCA cycle flux ($V_{tca}$) determined with NMR is equivalent to the rate of entry of acetyl coenzyme A

(acetyl CoA) into the TCA cycle according to the relationship

$$V_{tca} = V_g + V_\beta + V_{ac} \qquad (3)$$

where $V_g$, $V_\beta$, and $V_{ac}$ are the rates of acetyl CoA entry from glycolysis, β-hydroxybutyrate, and acetoacetate, respectively. Since each source of acetyl CoA generates different amounts of NADH and FAD, which are the compounds that link the TCA cycle to oxidative metabolism, the rate of oxygen consumption is different for each source. The $CMRo_2$ is given by the relationship

$$CMRo_2 = 3V_g + 2.25V_\beta + 2V_{ac} \qquad (4)$$

$V_g$ is assumed to be the difference between twice $CMR_{gl}$ and the rate of net lactate efflux [0.04 μmol min$^{-1}$ g$^{-1}$ (Knudsen et al., 1991)], so $V_g = 0.70 \pm 0.16$ μmol min$^{-1}$ g$^{-1}$ ($n = 4$). When the three rates of acetyl CoA formation are inserted, Eq. 4 yields a value of $2.14 \pm 0.48$ μmol min$^{-1}$ g$^{-1}$ for $CMRo_2$ ($5.07 \pm 1.14$ ml 100 g$^{-1}$ min$^{-1}$ at 37°C; $n = 4$), which is only 8% higher than 6 × $CMR_{gl}$ (Table 5) and approaches closely the stoichiometric relation

$$C_6H_{12}O_6 + 6O_2 \rightarrow 6CO_2 + 6H_2O$$
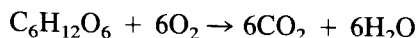
The present value of $CMRo_2$ agrees with previously published results from PET: LeBrun-Grandié et al. (1983), using PET, measured values of $5.41 \pm 1.30$ and $1.90 \pm 0.44$ ml 100 g$^{-1}$ min$^{-1}$ ($n = 19$) for $CMRo_2$ in 4-cm$^3$ volumes of the occipitoparietal cortex and white matter, respectively. If it is assumed that the value of $CMRo_2$ for the occipitoparietal cortex is purely a measurement in gray matter, then the NMR measurements of Gruetter et al. (1994) correspond to a tissue volume that consists of ~90% gray matter and ~10% white matter, which agrees closely with the previous calculation for $CMR_{gl}$.

The method is predicted to detect changes in oxygen consumption with a sensitivity similar to the 6–9% uncertainty of individual measurements of $V_{tca}$, including cases of broad changes in $CMRo_2$. As explained under Results, the limits of precise measurement of $V_{tca}$ lie between 7 and 300% of the normal value (0.05–2.25 μmol min$^{-1}$ g$^{-1}$). If no changes in relative substrate utilization occurred at

these extremes, the values would represent respective rates of oxygen utilization of 0.16–6.4 μmol min$^{-1}$ g$^{-1}$ (0.38–15 ml 100 g$^{-1}$ min$^{-1}$), which lie well beyond values of $CMRo_2$ expected in the human brain in vivo.

Changes in $CMRo_2$ can occur coincidentally with changes in relative substrate utilization, so we have determined the effect of substrate alterations on the determination of $CMRo_2$ from $V_{tca}$. If changes occur in $CMRo_2$ without alterations in the proportions of carbon substrates, the values of $CMRo_2$ will change exactly in proportion to $V_{tca}$. In some cases, however, the substrates utilized may change. For example, in diabetes ~50% of $CMRo_2$ can arise from ketone body utilization (Ruderman et al., 1974). If the utilization rates of β-hydroxybutyrate and acetoacetate are maintained relative to one another, Eqs. 3 and 4 indicate that such a fraction would represent 57% of $V_{tca}$ and would cause the measured enrichment of Glu C4 to be 13% instead of the present 27%. Since the measured enrichment represents only the glutamate that is actively turning over, the investigators would correctly ascribe the observed dilution to the utilization of unlabeled substrates, and the calculation of $V_{tca}$ and $CMRo_2$ would be correct. If, instead, the dilution arose entirely from unlabeled lactate utilization, the dilution would correspond to the unlikely lactate utilization rate of *three times* $CMR_{gl}$ but would yield an underestimate of only 16% in $CMRo_2$. In summary, cases of altered substrate utilization can be detected and quantified by measurement of the fractional Glu C4 enrichment and can be ascribed to the oxidation of acetate units via acetyl CoA with insignificant effects on the accuracy of the $CMRo_2$ determination.

### Exchange between α-KG and glutamate

The exchanges among the mitochondrial and cytosolic pools of α-KG and glutamate were mathematically equivalent to a single exchange between two pools described by $V_x$ (Mason et al., 1992a). One pool was the sum of the mitochondrial and cytosolic α-KG pools and the other was the sum of the mitochondrial and cytosolic glutamate pools. It was important to establish whether $V_x$ is fast or slow relative to the $V_{tca}$, since the exchange moves the isotopic label from the TCA cycle to glutamate and thereby enables the isotopic labeling of glutamate to be used as a measure of $V_{tca}$. Comparison of the glutamate C4 and glutamate C3 time courses yielded a value of $57 \pm 26$ for $V_x$ ($n = 3$), which is 72 times faster than $V_{tca}$. The high exchange rate is consistent with results in the rat brain (Balázs and Haslam, 1965; Balázs, 1970; Cooper and Meister,

**TABLE 5.** *The average values of* $V_{tca}$, $CMR_{gl}$, *and* $CMRo_2$ *(±SD; n = 4)*

| | Rate (μmol min$^{-1}$ g$^{-1}$) |
|---|---|
| $V_{tca}$ | $0.73 \pm 0.19$ |
| $CMR_{gl}$ | $0.37 \pm 0.08$ |
| $CMRo_2$ | $2.14 \pm 0.48$ |

1985; Hawkins et al., 1985; Mason et al., 1992a). The fast exchange rate is also consistent with the almost instantaneous equilibration of [$^{13}$N]ammonia into glutamate and aspartate in the rat liver in vivo (Cooper et al., 1987). The high rate of $\alpha$-KG/glutamate exchange means that glutamate is an excellent label trap and can be used for metabolic rate measurements in the human brain in vivo.

## Glutamine synthesis

The rate of glutamine synthesis ($V_{gln}$) was 0.47 $\mu$mol min$^{-1}$ g$^{-1}$, with a 95% confidence interval of 0.139–3.094 $\mu$mol min$^{-1}$ g$^{-1}$. The value of $V_{gln}$ was slightly less than the TCA cycle rate. The rate is higher than the value of 0.06–0.08 $\mu$mol min$^{-1}$ g$^{-1}$ (Kanamori et al., 1993; Kanamori and Ross, 1993) for the anesthetized rat brain but lower than the maximum activity of 0.7 $\mu$mol min$^{-1}$ g$^{-1}$ in the rat brain (Hawkins and Mans, 1983); the higher rate observed in the conscious human may be due to the effects of depolarization on glutamine synthesis. No measurements of glutamine synthesis rates in the human brain were available for comparison to the value determined by the model. Analysis of the sensitivity of the calculation of $V_{tca}$ showed that although the uncertainty in $V_{gln}$ was high, the value of $V_{gln}$ was high enough to accommodate a broad range of uncertainty with little effect on the value of $V_{tca}$.

## Compartmentation of the TCA cycle

Evidence exists that supports a model with two metabolic compartments of glutamate in the brain (for review see Cooper and Plum, 1987). One compartment contains a large pool of glutamate, and the other a small pool. Intracysternal injection of [$^{14}$C]glutamate and [$^{14}$C]glutamine into anesthetized monkeys showed that glutamine was more highly labeled than glutamate, which means that a small pool of glutamate must supply label to glutamine in the anesthetized monkey. Cooper et al. (1979, 1988) infused $^{13}$NH$_4^+$ into conscious rats and found that the $\alpha$-amino nitrogen of glutamine was more rapidly labeled than that of glutamate. Different isotopomer labeling patterns have been observed in the brains of anesthetized rats following [1,2-$^{13}$C]acetate (Cerdan et al., 1990). Also in anesthetized rats, brain glutamate and glutamine were both labeled and their C4 fractional enrichments differed from each other after infusions of either [U-$^{13}$C]$\beta$-hydroxybutyrate or [1,2-$^{13}$C]glucose (Künnecke et al., 1993). [1-$^{13}$C]Glucose perfusions of guinea pig brain slices caused labeling of glutamate and GABA without labeling of glutamine (Badar-Goffer et al., 1990), while in the presence of depolarizing levels of

KCl low fractions of glutamine were labeled (Badar-Goffer et al., 1992). All of the studies used brain slices or anesthetized animals. Since glutamine labeling increased with depolarization in brain slices, increased still more in intact anesthetized animals, and was the same as glutamate labeling in conscious humans, a certain degree of normal physiological activity may be necessary for complete labeling of the glutamine pool.

Mathematical models have been used to study cerebral metabolic compartmentation by analyzing radiolabeling data obtained in rats and mice (Garfinkel, 1966; Van den Berg and Garfinkel, 1971). While the present data do not distinguish metabolic compartments, the potential effects of compartmentation upon the interpretation of the data can be evaluated. The time course of $^{13}$C-labeled glutamate probably reflects the large glutamate pool, since in the rat brain the small pool is only 2–11% of the total glutamate concentration (Berl et al., 1961; Cooper et al., 1988), with a turnover time of ~1 min (Berl et al., 1961).

The time course of glutamine C4 slightly lags that of glutamate C4, so the data are consistent with three two-compartment possibilities: Glutamine is formed rapidly from (1) a large glutamate pool, (2) a small glutamate pool that is labeled rapidly, or (3) both glutamate compartments (Fig. 5). Since the data are consistent with all three extremes, the present data cannot distinguish among them. An exchange analysis similar to that in the appendix of Mason et al. (1992a) shows that for the rapid labeling of glutamine observed here, the value of $V_{tca}$
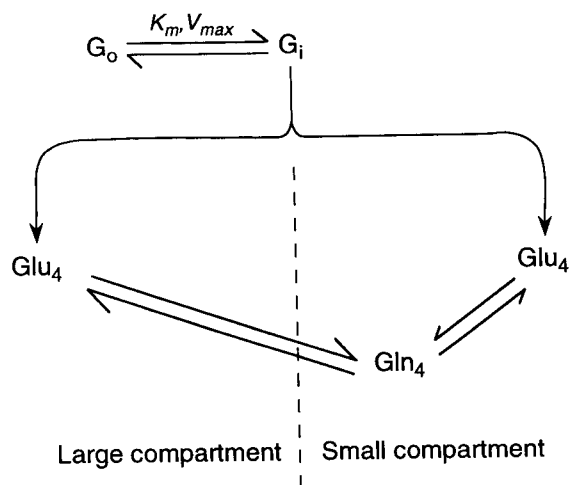
FIG. 5. Schematic of a two-compartment model for labeling of glutamate and glutamine. For the case in which labeling of glutamine C4 and glutamate C4 occur at nearly the same rate, this scheme is mathematically equivalent to the simpler scheme of Fig. 1.

derived from the present data varies negligibly among the three cases. The observed time course of glutamine C4 closely follows that of glutamate C4, so glutamine turns over almost as if it were part of the large pool of glutamate; the $[1-{}^{13}C]$glucose labels both pools approximately as if they composed a single pool. The data do not allow us to assign either the large or the small pool of glutamate as the precursor of glutamine. The sum of the rates of flow from $[1-{}^{13}C]$glucose into glutamate C4 and from the small pool of glutamate C4 into glutamine C4 must therefore be independent of the mechanism of label exchange between glutamine and the large pool of glutamate and can be represented mathematically as a single exchange reaction. A two-compartment analysis of these NMR data yields a combined pool value of $V_{tca}$ that is the sum of the rates of glutamate C4 labeling by $[1-{}^{13}C]$glucose and glutamine C4 labeling by the small glutamate pool. Since the small-pool $V_{tca}$ must be at least as fast as the rate of glutamine C4 labeling by the small pool, the combined pool value of $V_{tca}$ would be a minimum estimate. However, if glutamine labeling is slow or reduced in the system studied (e.g., brain slices or anesthetized brains), compartmentation may play an important role in the analysis of glutamate C4 time courses.

Since the values of $CMR_{gl}$ and $CMRo_2$ determined from our single-compartment analysis are in close agreement with previous measurements, the small pool of glutamate probably contributes negligibly to the total $V_{tca}$ in the human brain under the present conditions. The large pool is thought to represent neuronal glutamate metabolism (Van den Berg et al., 1970), so a similar $^{13}C$ NMR study of white matter might yield further information about compartmentation.

The values of $CMR_{gl}$ and $CMRo_2$ determined from our single-compartment analysis are in close agreement with previous measurements by PET and arterial–venous differences. The same analysis has been made in the past for rat brain data (Mason et al., 1992a), in which the $^{13}C$ turnover was measured by a POCE method (Rothman et al., 1985; Fitzpatrick et al., 1990). The POCE method has been applied to human brain studies (Rothman et al., 1992), and most recently it has been possible to obtain high-quality data from ~6 cm$^3$ of the brain, in contrast to the 144 cm$^3$ needed for $^{13}C$ measurements. Spectral resolution of the $^{13}C$ data has made it possible to validate the model and this method of data analysis. The present analysis can therefore be used confidently for interpreting human POCE data, which have a spatial resolution similar to that of measurements using PET.

## SUMMARY AND CONCLUSION

A mathematical model of human brain metabolism was used to analyze the $^{13}C$ isotopic labeling data of Gruetter et al. (1994), who infused $[1-{}^{13}C]$glucose and used $^{13}C$ NMR to observe the time courses of glutamate C4, glutamate C3, and glutamine C4. The model was fitted to the NMR data using the plasma glucose concentrations and $1-{}^{13}C$ fractional glucose enrichment time courses as input functions, and several metabolic rates were calculated. $V_{gln}$ was determined to be 0.47 µmol min$^{-1}$ g$^{-1}$, with 95% confidence intervals of 0.139–3.094 µmol min$^{-1}$ g$^{-1}$. $V_{tca}$ was 0.73 ± 0.19 µmol min$^{-1}$ g$^{-1}$ ($n = 4$). The individual uncertainties for $V_{tca}$ were much less than the intersubject variations, demonstrating that the $^{13}C$ NMR method is sensitive enough to measure intersubject variations. $V_x$ was 57 ± 26 µmol min$^{-1}$ g$^{-1}$ ($n = 3$), which is 72 times faster than $V_{tca}$. $CMR_{gl}$ was 0.37 ± 0.08 µmol min$^{-1}$ g$^{-1}$ ($n = 4$), and $CMRo_2$ was 2.14 ± 0.48 µmol min$^{-1}$ g$^{-1}$ (5.07 ± 1.14 ml min$^{-1}$ 100 g$^{-1}$; $n = 4$), which both agree with values previously reported for the occipital cortex. The glutamate data and the derived values apply predominantly to a large, presumably neuronal, pool of glutamate, and the glutamine data are compatible with either a one-compartment or a two-compartment analysis, providing that the model permits the rapid, complete labeling of glutamine that is observed in vivo.

## REFERENCES

Badar-Goffer RS, Bachelard HS, Morris PG (1990) Cerebral metabolism of acetate and glucose studied by $^{13}C$-n.m.r. spectroscopy: a technique for investigating metabolic compartmentation in the brain. *Biochem J* 266:133–139

Badar-Goffer RS, Ben-Yoseph O, Bachelard HS, Morris PG (1992) Neuronal-glial metabolism under depolarizing conditions—a $^{13}C$-n.m.r. study under depolarizing conditions. *Biochem J* 282:225–230

Balázs R (1970) Carbohydrate metabolism. In: *Handbook of Neurochemistry, Vol. 3* (Lajtha A, ed), New York, Plenum Press, pp 1–36

Balázs R, Haslam RJ (1965) Exchange transamination and the metabolism of glutamate in brain. *Biochem J* 94:131–141

Beckmann N, Turkalj I, Seelig J, Keller U (1991) $^{13}C$ NMR for the assessment of human brain glucose metabolism in vivo. *Biochemistry* 30:6362–6366

Behar KL, Petroff OAC, Prichard JW, Alger JR, Shulman RG (1986) Detection of metabolites in rabbit brain by $^{13}C$ NMR

spectroscopy following administration of [1-$^{13}$C]glucose. *J Magn Reson Med* 3:911–920

Berl S, Lajtha A, Waelsch H (1961) Amino acid and protein metabolism. VI. Cerebral compartments of glutamic acid metabolism. *J Neurochem* 7:186–197

Berl S, Takagaki G, Clarke DD, Waelsch H (1962) Carbon dioxide fixation in the brain. *J Biol Chem* 237:2570–2573

Cerdan S, Künnecke B, Seelig J (1990) Cerebral metabolism of [1,2-$^{13}$C]acetate as detected by *in vivo* and *in vitro* $^{13}$C NMR. *J Biol Chem* 265:12,916–12,926

Chance EM, Seeholzer SH, Kobayashi K, Williamson JR (1983) Mathematical analysis of isotope labeling in the citric acid cycle with applications to $^{13}$C NMR studies in perfused rat hearts. *J Biol Chem* 258:13,785–13,794

Cohen SM, Ogawa S, Shulman RG (1979) $^{13}$C NMR studies of gluconeogenesis in rat liver cells: utilization of labeled glycerol by cells from euthyroid and hyperthyroid rats. *Proc Natl Acad Sci USA* 76:1603–1607

Cohen SM, Rognstad R, Shulman RG, Katz J (1980) A comparison of $^{13}$C NMR and $^{14}$C tracer studies of hepatic metabolism. *J Biol Chem* 256:3428–3432

Cooper AJL, Meister A (1985) Metabolic importance of transaminases. In: *The Transaminases* (Metzler DE, Christen P, eds), New York, John Wiley, pp 533–536

Cooper AJL, Plum F (1987) Biochemistry and physiology of brain ammonia. *Physiol Rev* 67:440–519

Cooper AJL, McDonald JM, Gelbard AS, Gledhill RF, Duffy TE (1979) The metabolic fate of $^{13}$N-labeled ammonia in rat brain. *J Biol Chem* 254:4982–4992

Cooper AJL, Nieves E, Coleman AE, Filc-DeRicco S, Gelbard AS (1987) Short-term metabolic fate of [$^{13}$N]ammonia in rat liver *in vivo. J Biol Chem* 262:1073–1080

Cooper AJL, Lai CK, Gelbard AS (1988) Ammonia and energy metabolism in normal and hyperammonemic rat brain. In: *The Biochemical Pathology of Astrocytes* (Norenberg MD, Hertz L, Schousboe A, eds), New York, Liss, pp 419–434

Feinendegen LE, Herzog H, Wieler H, Patton DD, Schmid A (1986) Glucose transport and utilization in the human brain: model using carbon-11 methylglucose and positron emission tomography. *J Nucl Med* 27:1867–1877

Fitzpatrick SM, Hetherington HP, Behar KL, Shulman RG (1990) The flux from glucose to glutamate in the rat brain in vivo as determined by $^1$H-observed/$^{13}$C-edited NMR spectroscopy. *J Cereb Blood Flow Metab* 10:170–179

Gaitonde MK, Evison E, Evans GM (1983) The rate of utilization of glucose via hexosemonophosphate shunt in brain. *J Neurochem* 41:1252–1260

Garfinkel D (1966) A simulation study of the metabolism and compartmentation in brain of glutamate, aspartate, the Krebs cycle and related metabolites. *J Biol Chem* 241:3918–3929

Gottstein U, Bernsmeier A, Sedlmeyer I (1963) Der Kohlenhydratstoffwechsel des menschlichen Gehirns. I. Untersuchungen mit substratspezifischen enzymatischen Methoden bei normaler Hirndurchblutung. *Klin Wochenschrift* 41:943–948

Gruetter R, Novotny EJ, Boulware SD, Rothman DL, Mason GF, Shulman GI, Shulman RG, Tamborlane WV (1992a) Direct measurement of brain glucose concentrations in humans by $^{13}$C NMR spectroscopy. *Proc Natl Acad Sci USA* 89:1109–1112 (Erratum, 89:12,208)

Gruetter R, Rothman DL, Novotny EJ, Shulman RG (1992b) Localized $^{13}$C NMR spectroscopy of *myo*-inositol in the human brain *in vivo. Magn Reson Med* 25:204–210

Gruetter R, Novotny EJ, Boulware SD, Mason GF, Rothman DL, Prichard JW, Shulman RG (1994) Localized $^{13}$C NMR spectroscopy in the human brain of amino acid labeling from $^{13}$C glucose. *J Neurochem* 63:1377–1385

Hanstock CC, Rothman DL, Prichard JW, Jue T, Shulman RG (1988) Spatially localized $^1$H NMR spectra of metabolites in the human brain. *Proc Natl Acad Sci USA* 85:1821–1825

Hawkins RA, Mans AM (1983) Intermediary metabolism of carbohydrates and other fuels. In: *Handbook of Neurochemis-*

*try, Vol. 3* (Lajtha A, ed), New York, Plenum Press, pp 259–294

Hawkins RA, Mans AM, Davis DW, Viña JR, Hibbard LS (1985) Cerebral glucose use measured with [$^{14}$C]glucose labeled in the 1, 2, or 6 position. *Am J Physiol* 248:C170–C176

Heiss W-D, Pawlik G, Herholz K, Wagner R, Göldner H, Weinhard K (1984) Regional kinetic constants and cerebral metabolic rate for glucose in normal human volunteers determined by dynamic positron emission tomography of [$^{18}$F]-2-fluoro-2-deoxy-D-glucose. *J Cereb Blood Flow Metab* 4:212–223

Howse DC, Duffy TE (1975) Control of the redox state of the pyridine nucleotides in the rat cerebral cortex. Effect of electroshock-induced seizures. *J Neurochem* 24:935–940

Juhlin-Dannfelt A (1977) Ethanol effects of substrate utilization by the human brain. *Scand J Clin Lab Invest* 37:443–449

Kanamori K, Ross BD (1993) $^{15}$N n.m.r. measurement of the *in vivo* rate of glutamine synthesis and utilization at steady state in the brain of the hyperammonemic rat. *Biochem J* 293:461–468

Kanamori K, Parivar F, Ross BD (1993) A $^{15}$N NMR study of in vivo cerebral glutamine synthesis in hyperammonemic rats. *NMR Biomed* 6:21–26

Katz J, Rognstad R (1976) Futile cycles in the metabolism of glucose. *Curr Topics Cell Regul* 10:237–289

Knudsen GM, Paulson OB, Hertz MM (1991) Kinetic analysis of the human blood-brain barrier transport of lactate and its influence by hypercapnia. *J Cereb Blood Flow Metab* 11:581–586

Künnecke B, Cerdan S, Seelig J (1993) Cerebral metabolism of [1,2-$^{13}$C$_2$]glucose and [U-$^{13}$C$_4$]3-hydroxybutyrate in rat brain as detected by $^{13}$C NMR spectroscopy. *NMR Biomed* 6:264–277

Lebrun-Grandié P, Baron J-C, Soussaline F, Loch'h C, Sastre J, Bousser M-G (1983) Coupling between regional blood flow and oxygen utilization in the normal brain: a study with positron tomography and oxygen 15. *Arch Neurol* 40:230–236

Lowry OH, Passonneau JV (1964) The relationship between substrates and enzymes of glycolysis in brain. *J Biol Chem* 239:31–42

Malloy CR, Sherry AD, Jeffrey FMH (1990a) Analysis of tricarboxylic acid cycle of the heart using $^{13}$C isotope isomers. *Am J Physiol* H987–H996

Malloy CR, Thompson JR, Jeffrey FMH, Sherry AD (1990b) Contribution of exogenous substrates to acetyl coenzyme A: measurement by $^{13}$C NMR under non-steady-state conditions. *Biochemistry* 29:6756–6761

Mason GF, Rothman DL, Behar KL, Shulman RG (1992a) NMR determination of the TCA cycle rate and α-ketoglutarate/glutamate exchange rate in rat brain. *J Cereb Blood Flow Metab* 12:434–447

Mason GF, Behar KL, Rothman DL, Shulman RG (1992b) NMR determination of intracerebral glucose concentration and transport kinetics in rat brain. *J Cereb Blood Flow Metab* 12:448–455

Pardridge WM, Oldendorf WH (1977) Transport of metabolic substrates through the blood-brain barrier. *J Neurochem* 28:5–12

Petroff OAC, Spencer DD, Alger JR, Prichard JW (1989) High-field proton magnetic resonance spectroscopy of human cerebrum obtained during surgery for epilepsy. *Neurology* 39:1197–1202

Phelps ME, Huang SC, Hoffman EJ, Selin C, Sokoloff L, Kuhl DE (1979) Tomographic measurement of local cerebral glucose metabolic rate in humans with (F-18)2-fluoro-2-deoxy-D-glucose: Validation of method. *Ann Neurol* 6:371–388

Rapoport SI (1991) Discussion of PET workshop reports, including recommendations of PET data analysis working group. *J Cereb Blood Flow Metab* 11:A140–A146

Rothman DL, Behar KL, Hetherington HP, den Hollander JA, Bendall MR, Petroff OAC, Shulman RG (1985) $^1$H-observed/$^{13}$C-decoupled spectroscopic measurement of lactate and

glutamate in the rat brain *in vivo*. *Proc Natl Acad Sci USA* 82:1633–1637

Rothman DL, Novotny EJ, Shulman GI, Howseman AM, Petroff OAC, Mason GF, Nixon T, Hanstock CC, Prichard JW, Shulman RG (1992) $^1$H-[$^{13}$C] NMR measurements of [4-$^{13}$C]-glutamate turnover in human brain. *Proc Natl Acad Sci USA* 89:9603–9606

Ruderman NB, Ross PS, Berger M, Goodman MN (1974) Regulation of glucose and ketone-body metabolism in brain of anesthetized rats. *Biochem J* 138:1–10

Shulman GI, Rothman DL, Jue T, Stein P, DeFronzo RA, Shulman RG (199) Quantitation of muscle glycogen synthesis in normal subjects and subjects with non-insulin-dependent diabetes by $^{13}$C nuclear magnetic resonance spectroscopy. *N Engl J Med* 322:223–228

Tyler JL, Strother SC, Zatorre RJ, Alivisatos B, Worsley KJ,

Diksie M, Yamamoto YL (1988) Stability of regional cerebral glucose metabolism in the normal brain measured by positron emission tomography. *J Nucl Med* 29:631–642

Van den Berg CJ, Garfinkel D (1971) A simulation study of brain compartments: metabolism of glutamate and related substances in mouse brain. *Biochem J* 123:211–218

Van den Berg CJ, Kržalić LJ, Mela P, Waelsch H (1970) Compartmentation of glutamate metabolism in brain: Evidence for the existence of two different tricarboxylic acid cycles in brain. *Biochem J* 113:281–290

Vyska K, Magloire JR, Freundlieb C, Höck A, Becker V, Schmid A, Feinendegen LE, Kloster G, Stöcklin G, Schuier FJ, Thal HU (1985) In vivo determination of the kinetic parameters of glucose transport in the human brain using $^{11}$C-methyl-D-glucose (CMG) and dynamic positron emission tomography (dPET). *Eur J Nucl Med* 11:97–106